



Incorporation of bioactive glass nanoparticles in electrospun PCL/chitosan fibers by using benign solvents



Liliana Liverani^a, Jonas Lacina^a, Judith A. Roether^b, Elena Boccardi^a, Manuela S. Killian^c, Patrik Schmuki^{c,d}, Dirk W. Schubert^b, Aldo R. Boccaccini^{a,*}

^a Institute of Biomaterials, Department of Materials Science and Engineering, University of Erlangen-Nuremberg, Cauerstr. 6, 91058 Erlangen, Germany

^b Institute of Polymeric Materials, Department of Materials Science and Engineering, University of Erlangen-Nuremberg, Martensstrasse 7, 91058 Erlangen, Germany

^c LKO, Department of Materials Science and Engineering, University of Erlangen-Nuremberg, Martensstrasse 7, 91058 Erlangen, Germany

^d Department of Chemistry, King Abdulaziz University, Jeddah, Saudi Arabia

ARTICLE INFO

Article history:

Received 5 December 2016

Received in revised form

7 May 2017

Accepted 9 May 2017

Available online 17 May 2017

Keywords:

Green electrospinning

Benign solvents

Bioactive glass

Composite

PCL

Chitosan

Nanofibers

ABSTRACT

The use of bioactive glass (BG) particles as a filler for the development of composite electrospun fibers has already been widely reported and investigated. The novelty of the present research work is represented by the use of benign solvents (like acetic acid and formic acid) for electrospinning of composite fibers containing BG particles, by using a blend of PCL and chitosan. In this work, different BG particle sizes were investigated, namely nanosized and micron-sized. A preliminary investigation about the possible alteration of BG particles in the electrospinning solvents was performed using SEM analysis. The obtained composite fibers were investigated in terms of morphological, chemical and mechanical properties. An *in vitro* mineralization assay in simulated body fluid (SBF) was performed to investigate the capability of the composite electrospun fibers to induce the formation of hydroxycarbonate apatite (HCA).

© 2017 The Authors. Production and hosting by Elsevier B.V. on behalf of KeAi Communications Co., Ltd. This is an open access article under the CC BY-NC-ND license (<http://creativecommons.org/licenses/by-nc-nd/4.0/>).

1. Introduction

The electrospinning technique has been widely used for the fabrication of nano and micronsized fibers for numerous applications in the biomedical field, including tissue engineering scaffolds. The principle for the obtainment of a fibrous mesh starting from a polymeric solution (or blend or melt) is based on the application of a high intensity electric field between two electrodes of opposite polarity. The standard setup is composed of a high voltage generator, a syringe pump comprising either a needle or small capillary, controlling the flow rate of polymeric solution extrusion and a grounded or negatively charged fiber collector [1–4]. The electrospinning process parameters may be grouped into three categories, namely solution properties, process parameters and environmental parameters. The investigation of these categories and their

influence on the final properties of the obtained fibrous mats have been widely scrutinized in literature [5]. Among them, the selection of the solvent plays a pivotal role [6,7]. Besides the importance and the influence of the solvent on fiber morphology and roughness, the presence of possible residuals inside the obtained samples could limit their application in the biomedical field or require post-processing to remove these (often toxic) residuals. The use of benign solvents, as well as modified techniques such as suspension or emulsion electrospinning are some examples of “green” electrospinning according to its definition [8,9].

Poly(ϵ -caprolactone) (PCL) is a polyester widely investigated for biomedical applications due to its interesting properties including biocompatibility, biodegradability and possessing FDA approval for clinical use [10–12]. PCL has been processed by electrospinning ever since the more widespread use of this technique. It has mainly been electrospun using chloroform, dichloromethane, dimethylformamide and methanol or a mixture of the above [13,14], but also positive results have been reported about electrospinning of PCL using less optimal solvents, like acetic acid, formic acid and acetone [11,15–17]. Chitosan is a polysaccharide widely used for

* Corresponding author.

E-mail address: aldo.boccaccini@ww.uni-erlangen.de (A.R. Boccaccini).

Peer review under responsibility of KeAi Communications Co., Ltd.

biomedical applications, because of its biocompatibility, biodegradability and antibacterial properties [18]. The electrospinning of chitosan is a challenging issue, in particular if the use of toxic organofluorine solvents is avoided, for this reason it is commonly electrospun in a blend with synthetic polymers like poly vinyl alcohol (PVA) or poly ethylene oxide (PEO) [19,20].

The use of composite materials and in particular electrospun composites for biomedical applications has been widely investigated to combine the properties of the organic matrix with the reinforcement of the inorganic phase embedded inside the fibers [21].

The fabrication of electrospun composites using benign solvents has been recently achieved in different research works reporting interesting and promising results [22–24].

The aim of the present research work is to fabricate composite electrospun PCL/chitosan nanofibers by using benign solvents. For the selection of the inorganic phase, bioactive glass (BG) (45S5 Bioglass® composition) was selected for its well-known effects on osteogenesis, angiogenesis and its antibacterial activity. Two different BG sizes were investigated and compared. Morphological, chemical and mechanical properties as well as acellular bioactivity of the obtained composite fibers were investigated for both BG particle sizes.

2. Materials and methods

2.1. Solution preparation

Electrospun mats were obtained from poly(epsilon-caprolactone) (PCL) (80 kDa, Sigma Aldrich, Germany) and chitosan (CS) (medium molecular weight, molecular weight 190,000–310,000 Da and degree of deacetylation 75–85%, Sigma Aldrich, Germany) solutions. Acetic acid (AA, VWR, Germany) and formic acid (FA, VWR Chemicals, Germany) were used as solvents.

An optimization of the protocol reported in Ref. [25] was performed. Briefly, chitosan was added to a solution containing 6% w/v of PCL in a mixture of formic acid and acetic acid in the ratio of 7:3 in a weight ratio of 20% with respect to the amount of PCL. The solution of PCLCS was stirred for 72 h.

For the fabrication of the composite electrospun mats, commercially available BG particles (Schott Vitryxx®, nominal mean particle size 2 µm), labelled mBG, and 45S5 bioactive glass nanoparticles, labelled nBG (SSA: 52 m²/g, nominal particle size in the range 20–80 nm, developed at ETH Zurich) fabricated using flame-spray synthesis [26,27], were homogeneously dispersed in the polymer blend solution (30 wt% with respect to polymer amount), by constant stirring for 10 min and subsequent immersion in ultrasonic bath for 1 min, before electrospinning.

2.2. Electrospinning process

The optimized electrospinning parameters for the solution of neat PCLCS and PCLCS containing BG particles were kept constant in order to perform a comparative analysis of the obtained mats. The selected values were an applied voltage of 20 kV, a needle-target distance of 12.5 cm, while the polymeric solution was fed in using a flow rate of 0.3 mL/h and a needle diameter of 21G. Environmental parameters (temperature (T) and relative humidity (RH)) were checked and kept in the range T: 23–26 °C and RH: 35–50%. Electrospinning was performed using a commercially available setup (Starter Kit 40 KV Web, Linari srl, Italy).

2.3. Characterization

Samples morphology was assessed by SEM analysis (FE-SEM

(Auriga, Carl-Zeiss, Germany)). Samples were sputtered with gold before SEM analysis using a Sputter Coater (Q150T, Quorum Technologies). Fiber average diameters were calculated using ImageJ analysis software (NIH, USA), after the measurement of 50 fibers from each sample.

FTIR spectra of selected samples were obtained using an FTIR spectrometer (Nicolet 6700, Thermo Scientific, Germany) in attenuated total reflectance mode (ATR). For the analysis, 32 spectral scans at a resolution of 4 cm⁻¹ were repeated over the wavenumber range 4000–550 cm⁻¹. For the BG powder, KBr pellets were fabricated, by dispersing the sample in KBr, and the measurements were performed in the wavenumber range 4000–400 cm⁻¹. The used window material was CsI.

The PCL/chitosan (blend) samples were characterized by ToF-SIMS analysis (ToF.SIMS V, IONTOF, Münster) to confirm the presence of chitosan and characterize its distribution in the electrospun mats. Spectra were recorded on 7 spots (100 × 100 µm) per sample, images on 3 spots (250 × 250 µm) in high spectral resolution mode (m/Δm > 8000 at ²⁹Si) to avoid overlap of the signals, using a pulsed 25 keV Bi³⁺ beam. Low energy electron flooding in between measurements was used to prevent charging of the samples. Signals were identified using the accurate mass as well as their isotopic pattern. Poisson correction was used for integration of the signal intensities. Positive polarity spectra were normalized to their total intensity and calibrated on CH₃⁺, C₂H₃⁺, C₃H₅⁺, C₄H₉⁺ and C₇H₇⁺.

The mechanical characterization of selected fibrous mats was performed by uniaxial tensile strength tests using a universal testing machine (K. Frank GmbH, Germany) at room temperature. The measurements were carried out at a crosshead speed of 10 mm/min using a 50 N load cell. In order to correctly handle the electrospun mats, avoiding the application of any pretension on the samples before the mechanical tests, the use of a suitable paper square framework was necessary. The samples were cut into a rectangular shape of 5 mm wide and 4 cm long with the internal length of the paper framework being 2 cm.

The thermal degradation of the fibers was measured using thermogravimetric analysis (TGA) with the thermo-gravimetric analyzer Q5000IR (TA instruments, USA). The temperature was varied from 25° to 600 °C at a rate of 10 °C/min. Inert nitrogen atmosphere was used. TGA analysis was performed to investigate the possible effects of the presence of chitosan in the blend PCL/chitosan electrospun mats and to assess the incorporation of BG particles in the electrospun mats.

The acellular bioactivity of the electrospun composite samples containing BG was evaluated by immersion of the samples inserted in suitable scaffold holders (CellCrown™ 24, Scaffoldex, Sigma Aldrich, Germany) in a simulated body fluid (SBF) solution, according to an existing protocol [28], for 1, 3 and 7 days. A falcon tube containing SBF as a control was incubated for the entire period of the experiment to control overtime the stability of the testing solution.

After immersion, samples were characterized by SEM and ATR-FTIR analyses. The pH in the SBF solution was also investigated for each time point. The bioactivity of the samples was related to the formation of the hydroxyapatite phase on the surface of samples upon immersion in SBF [28]. The deposition of this layer was also characterized by XRD analysis (XRD, Miniflex 600, Rigaku, range 2θ: 10–60°, step 0.02, 4 deg/min, 40 kV, 15 mA).

Degradation tests after the immersion in PBS were also performed to confirm that the changes in the samples observed by SEM analysis after being immersed in SBF solution were not related to sample degradation. Samples were immersed in phosphate buffered saline (PBS) solution (Amresco LLC, USA) for 1 day at 37 °C using scaffold holders (CellCrown™ 24, Scaffoldex, Sigma Aldrich, Germany), as described above.

In order to investigate the possible effects of the electrospinning solvents on the BG particles, both particulate samples, mBG and nBG, were placed directly into the solution with the same ratio of solvents as used in the experiments (i.e. without polymers). After 10 min of constant stirring, the solutions were dipped in an ultrasonic bath for 1 min. After 20 min, the suspension was centrifuged (7000 rcf, 20 °C) for 10 min. After removing the supernatant, the particles were washed with deionized water and centrifuged three times using the same parameters. The particles were then dried at 60 °C for 48 h.

3. Results and discussion

3.1. Effects of immersion of BG particles in benign solvents

The immersion of BG particles in the solvents used for electrospinning was performed to assess any possible modifications occurring due to immersion (without any polymers in the solution). Even if it is not commonly investigated, the stability of bioactive glass particles in electrospinning solvents plays a pivotal role. In fact, as reported by Cerruti et al. [29], the pH of the solution could affect BG reactivity. In particular in a low pH solution, a total breakdown of the glassy network could occur, resulting in the absence of phosphate precipitation.

SEM micrographs, reported in Fig. 1, showed that for both BG particles slight morphological modifications occurred. In particular in case of the micron-sized particles several cracks are visible on the surface of the particles (Fig. 1B), but the particle size was not altered. In the case of nBG (Fig. 1D), the particles look more aggregated and compact compared to the sample before immersion (Fig. 1C).

3.2. Optimization of PCLCS parameters

The use of the mixture of formic acid and acetic acid for the electrospinning of the blend of PCL and chitosan has already been reported by Van der Schueren et al. [25]. In the present work, the

Table 1

Sample composition, sample labels and calculated average fiber diameters.

Sample	Sample label	Average fiber diameter (nm)
PCL/chitosan	PCLCS	57 ± 24
PCL/chitosan with 30 wt% mBG	PCLCS_mBG	95 ± 105
PCL/chitosan with 30 wt% nBG	PCLCS_nBG	74 ± 41

optimization of this protocol has been accomplished, i.e. the high voltage value as well as the solution flow rate and the needle inner diameter were decreased. By optimizing these parameters, beadless fibrous mats were obtained. The average fiber diameter of the blend electrospun mats thus becomes four times smaller than the value reported in literature, as reported in Table 1. Moreover, composite fibrous meshes comprising nBG and mBG particles were fabricated. The amount of BG particles was selected according to the literature [23] and fixed at 30 wt% with respect to the polymer amount, in order to obtain phosphate precipitation on the electrospun mats. Incorporation of BG particles was investigated and confirmed by SEM/EDX analysis, as reported in Fig. 2. SEM micrographs obtained at lower magnification (Fig. 2A and B) showed the distribution of the particles indicating that particles aggregated inside the electrospun mats.

No significant differences were detected in the calculation of the average fibers diameters, summarized in Table 1. Merely a slight increase in average values, after the addition of BG particles of both sizes could be noted. Another difference that could be detected in the samples containing BG particles was the increase of the standard deviation, in fact due to the increase in the conductivity of the polymeric solution containing BG particles, the range of minimum and maximum fiber diameter became wider.

FTIR analysis was used for the characterization of the obtained blend electrospun mats and composite mats. Due to the prevalence of PCL with respect to the amount of chitosan, the FTIR spectrum of electrospun neat PCL fibers is also shown in Fig. 3, as a comparison. In Table 2, a summary of all the main bands with the indications of the assignment is provided.

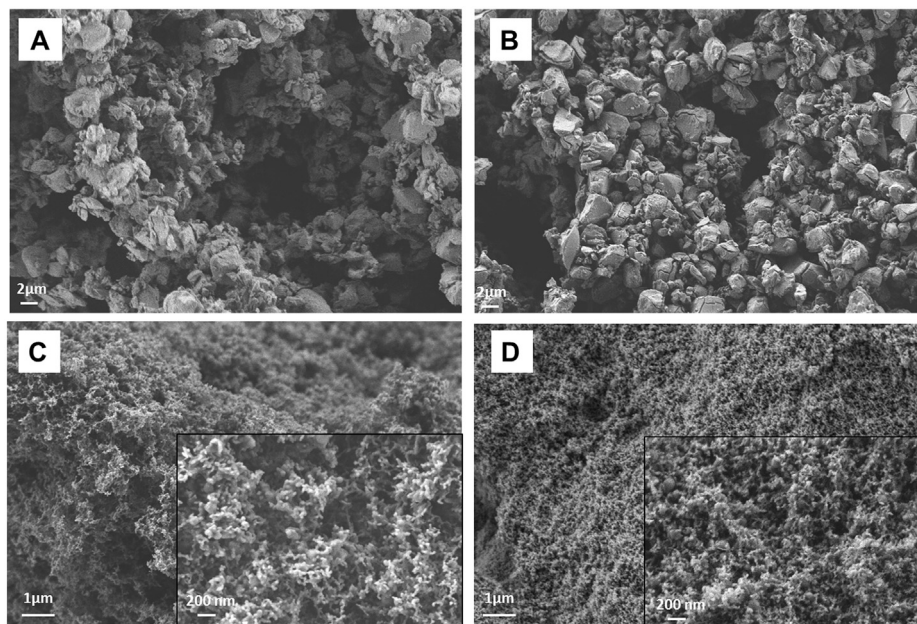


Fig. 1. SEM micrographs of mBG particles before (A) and after (B) immersion in the mixture of electrospinning solvents and nBG particles before (C) and after (D) immersion in the mixture of electrospinning solvents. Due to different particle sizes, different magnifications are reported (5kX, scale bar 2 µm for A and B and 20kX, scale bar 1 µm for C and D, insets in C and D: 80kX scale bar 200 nm).

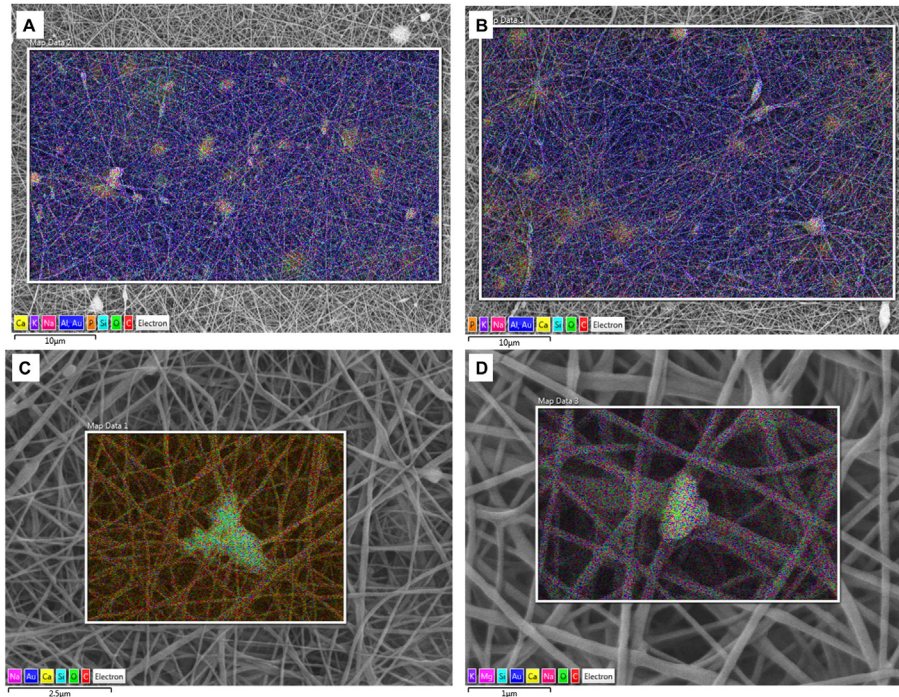


Fig. 2. SEM/EDX images, confirming the presence of BG particles of samples PCLCS_mBG (A, C) and PCLCS_nBG (B, D).

The main bands ascribable to PCL, like the peaks at 2949 and 2865 cm^{-1} , due to the asymmetric and symmetric CH_2 stretching, the peak centered at 1720 cm^{-1} ascribable to carbonyl stretching, could be identified in all the spectra of the blend and composite electrospun mats reported in Fig. 3 [30]. The presence of chitosan in the blend and composite electrospun mats is confirmed by the presence of the broad band centered at around 3435 cm^{-1} ascribable to OH and NH stretching of chitosan and by the band centered at 1590 cm^{-1} attributed to amide II bands of chitosan [25]. All these bands are not detected in the FTIR spectrum of electrospun neat PCL. The presence of BG particles, for both nBG and mBG, could be detected by the appearance of the bands centered at around

1100 cm^{-1} , ascribable to Si–O–Si symmetric stretching and the peak at 800 cm^{-1} due to $\delta(\text{Si–O–Si})$ [27].

The composition of the electrospun fibers was assessed with time-of-flight secondary ion mass spectrometry (ToF-SIMS). Spectra of PCL and PCLCS were compared according to the signals reported for PCL and chitosan in the study of Tortora et al. [32]. The nitrogen containing fragments m/z 18.03 - NH_4^+ , 30.03 - CH_4N^+ , 60.04 - $\text{C}_2\text{H}_6\text{NO}^+$, 73.05 - $\text{C}_3\text{H}_7\text{NO}^+$, 96.04 - $\text{C}_5\text{H}_6\text{NO}^+$, 100.04 - $\text{C}_4\text{H}_6\text{NO}_2^+$, 112.04 - $\text{C}_5\text{H}_6\text{NO}_2^+$ and 144.07 - $\text{C}_6\text{H}_{10}\text{NO}_3^+$ were assigned to chitosan and all of them appear predominantly on the PCLCS sample. The most intense of these fragments, NH_4^+ and CH_4N^+ , are displayed in Fig. 4A for both PCL and PCLCS. Fig. 4B shows the

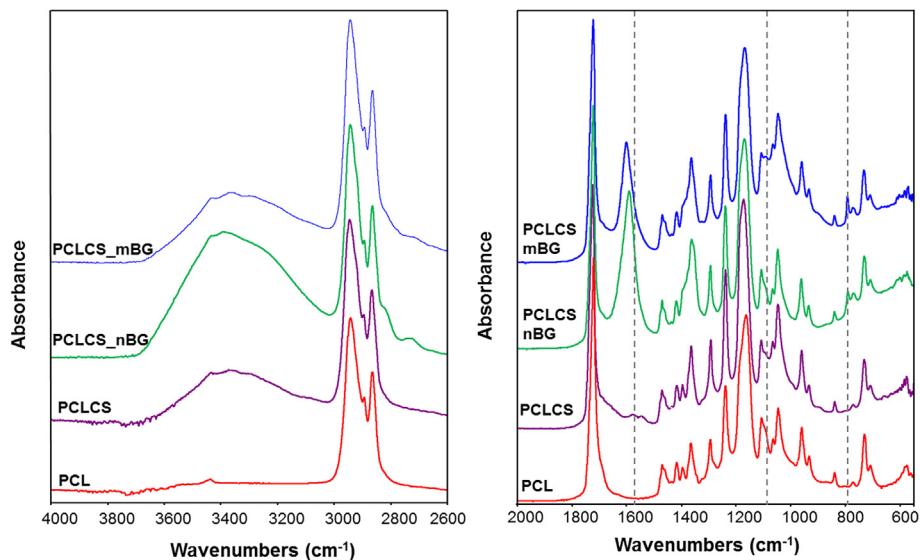
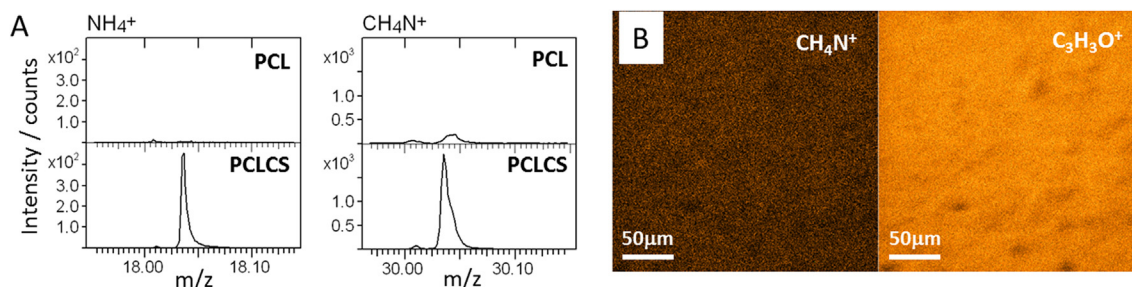


Fig. 3. FTIR spectra for the electrospun PCL, electrospun blend PCLCS, electrospun composites PCLCS_nBG and PCLCS_mBG.

Table 2

Overview of the main bands detected in FTIR spectra of electrospun PCL, electrospun PCLCS and electrospun composites PCLCS_nBG and PCLCS_mBG.

Wavenumber (cm ⁻¹)	Assignment	Abbreviation	References
3435	overlapping OH & NH stretching vibration due to chitosan	$\nu(\text{OH} \& \text{NH})/\nu(\text{OH})$	[25]
-2949	asymmetric CH ₂ stretching	$\nu_{\text{as}}(\text{CH}_2)$	[30]
-2865	symmetric CH ₂ stretching	$\nu_{\text{s}}(\text{CH}_2)$	[30]
-1720	carbonyl stretching	$\nu(\text{C}=\text{O})$	[30]
-1590	amide II bands of chitosan	$\nu(\text{NH})$	[25]
-1460	symmetrically coordinated pure CO ₃ ²⁻ ions	$\nu_3(\text{CO}_3^{2-})$	[27]
-1293	C–O & C–C stretching in the crystalline phase	ν_{cr}	[30]
-1238	asymmetric COC stretching	$\nu_{\text{as}}(\text{COC})$	[30]
1000–1200	Si–O–Si bond	$\nu(\text{Si–O–Si})$	[27]
-1166	symmetric COC stretching	$\nu_{\text{s}}(\text{COC})$	[30]
-1000	Si–OH symmetric stretching (after immersion in SBF)	$\nu(\text{Si–OH})$	[31]
-800	bending Si–O–Si	$\delta(\text{Si–O–Si})$	[27]
600	PO bending (after immersion in SBF)	$\delta(\text{PO})$	[31]
560	PO bending (after immersion in SBF)	$\delta(\text{PO})$	[31]

**Fig. 4.** ToF-SIMS spectral regions of chitosan characteristic fragments NH_4^+ and CH_4N^+ on PCL and PCLCS samples (A) and chemical mapping of PCLCS, showing the distribution of CH_4N^+ (chitosan) and $\text{C}_3\text{H}_3\text{O}^+$ (PCL) (B).

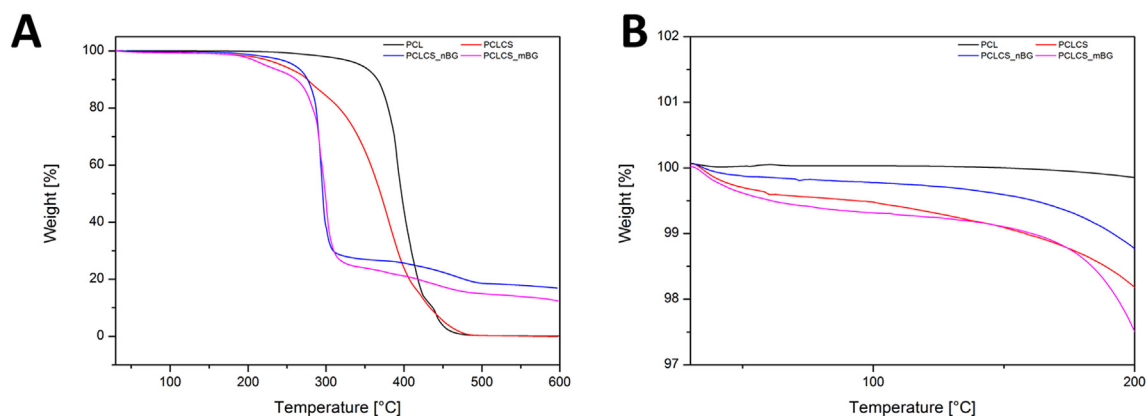
mapping of chitosan (CH_4N^+) on the PCL matrix ($\text{C}_3\text{H}_3\text{O}^+$), chitosan is seen to be homogeneously distributed over the whole fiber surface.

TGA analysis was performed on neat PCL, blend PCLCS and composite electrospun mats. The obtained thermogravimetric curves are reported in Fig. 5. The results confirm that the presence of chitosan affects the thermal properties of neat PCL electrospun mats. In fact, according to Noor Aliah et al. [33] the neat PCL fibers showed a single step trend, while for the blend PCLCS a two-step trend could be detected in Fig. 5B. According to the literature [33,34], the temperature corresponding to 50% sample weight loss was selected for the comparison among all the samples. Neat PCL fibers showed the highest value, around 400 °C, this value decreases for the blend PCLCS sample

(around 370 °C), while both the composites PCLCS_nBG and PCLCS_mBG show lower and comparable values (around 300 °C). After the polymeric blend decomposition, the residual weight is due to the presence of BG particles and the amount is comparable to the initial amount introduced in the suspension. Moreover, no significant differences between the two composite samples were measured, confirming that the particle size does not affect the incorporation of BG particles in electrospun mats.

3.3. Acellular bioactivity test

The composite samples were immersed in SBF solution to test their bioactivity. The electrospun sample without BG particles was

**Fig. 5.** Thermogravimetric curves for electrospun mats of neat PCL, blend of PCL and chitosan (PCLCS) and the composites PCLCS_mBG and PCLCS_nBG (A) and zoom view in the range 25–200 °C (B).

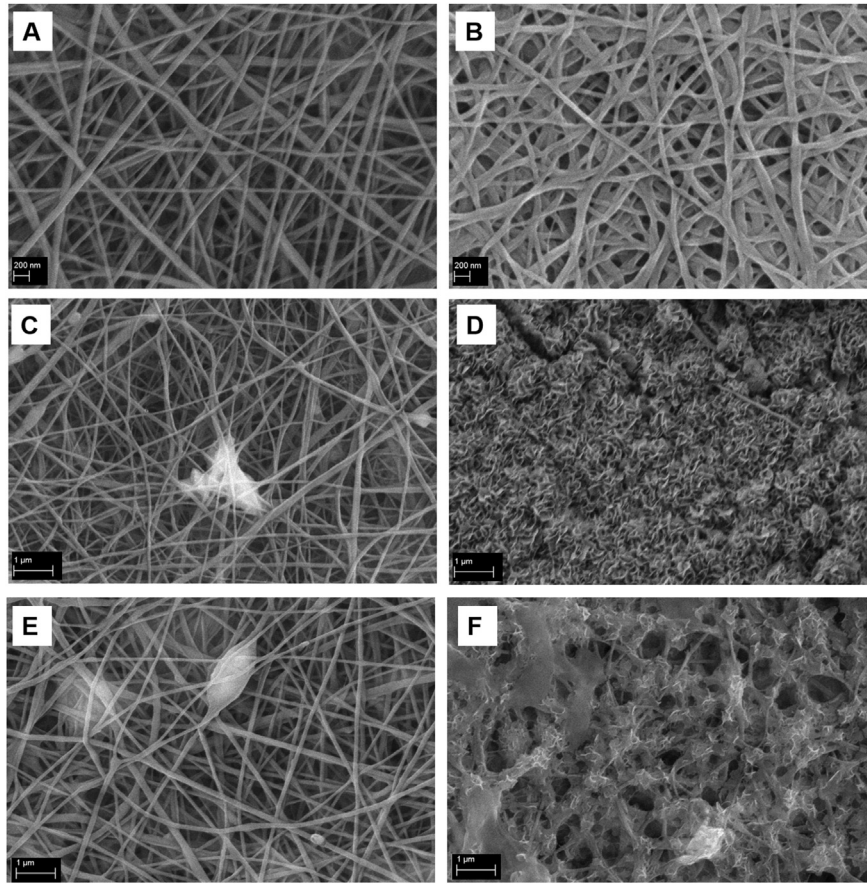


Fig. 6. SEM micrographs of electrospun PCLCS samples before (A) and after 7 days of immersion in SBF solution (B); PCLCS_mBG sample before (C) and after 7 days of immersion in SBF solution (D); PCLCS_nBG sample before (E) and after 7 days of immersion in SBF solution (F).

also immersed in SBF solution, as a control. After 7 days of immersion in SBF solution, no deposits could be observed on the blend PCLCS sample used as the control (Fig. 6B). On the contrary, hydroxycarbonate apatite (HCA) deposition could be observed on both composites obtained by the addition of mBG (Fig. 6D) and nBG (Fig. 6F).

Because of the differences in the morphology of the deposits noticed on sample PCLCS_nBG (Fig. 6F) after 7 days of immersion in SBF solution, with respect to the analogous sample PCLCS_mBG

(Fig. 6D) showing the typical and widely reported cauliflower-structure, PCLCS_nBG sample was investigated in detail with EDX, as reported in Fig. 7. From EDX analysis, it was possible to detect the presence of calcium and phosphorus in the sample after immersion in SBF solution.

In order to assess any possible morphological modification introduced by the immersion in a buffered solution, the composite samples were also immersed in PBS solution. The blend sample PCLCS was also immersed and used as a control. SEM analysis of

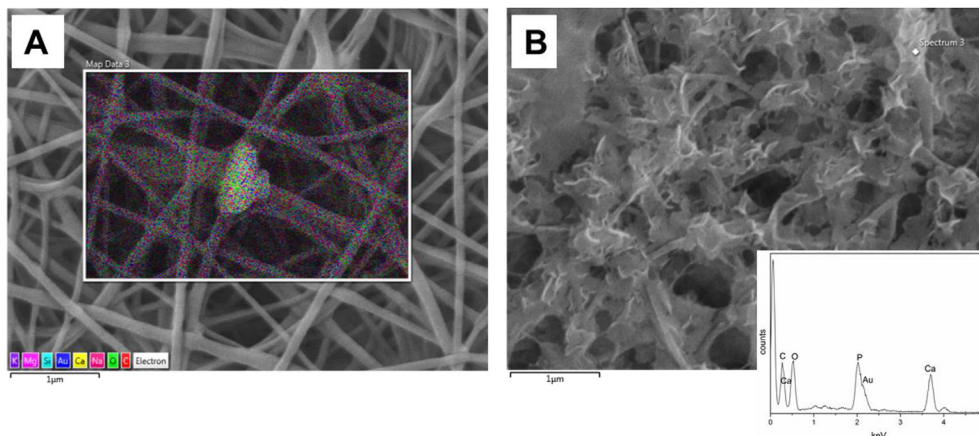


Fig. 7. SEM and EDX analysis on PCLCS_nBG electrospun sample before immersion in SBF (A) and after 7 days immersion in SBF (B).

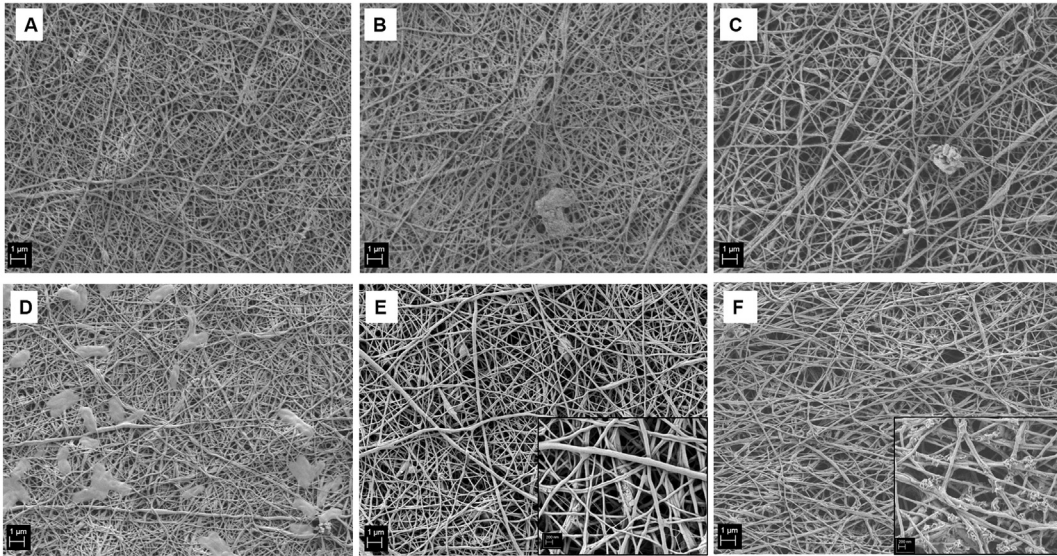


Fig. 8. SEM micrographs of electrospun PCLCS (A), PCLCS_mBG (B) and PCLCS_nBG (C) after immersion in PBS solution for 1 day and electrospun PCLCS (D), PCLCS_mBG (E) and PCLCS_nBG (F) after immersion in SBF solution for 1 day (magnification 10kX scale bar 1 μm and for the inlet magnification 45kX scale bar 200 nm).

the immersed samples, reported in Fig. 8, highlights that no relevant differences or deposits could be detected in the polymeric blend sample and in both composite samples, in particular in comparison with the same samples after immersion in SBF at the same time point, confirming that the morphological modifications detected after immersion in SBF could not be ascribable to the immersion in a buffered solution, but they are related to sample mineralization.

To assess and investigate deposit formation on the electrospun composite fibers, FTIR analysis was used for the evaluation of the samples after immersion in SBF and PBS solution, FTIR spectra of the samples are reported in Fig. 9. Samples were immersed in PBS solution for 1 day, because as reported in the FTIR spectra, already after 1 day of immersion in SBF solution evidence of the HCA deposition could be detected.

In particular in the composite samples (PCLCS_mBG and PCLCS_nBG) the peaks related to the phosphate group vibrations

could be noticed already after 1 day of immersion and there are no significant differences between the FTIR spectra after 1 day or 7 days of immersion in SBF. In detail, peaks at 560 and 600 cm^{-1} attributed to phosphate group vibrations, as reported in Table 2, could be detected in both composites already after 1 day of immersion in SBF solution, while these bands could not be detected in the same samples immersed in PBS solution for 1 day. Moreover, the band centered around 1000 cm^{-1} , ascribable to Si–OH stretching vibration could be noticed in the spectra of both composites already after 1 day of immersion in SBF solution. No differences are detected among the FTIR spectra of the polymeric blend sample before and after immersion in PBS or SBF solution (Fig. 9A).

XRD analysis was performed to characterize the deposition observed by SEM on composite fibers, reported in Fig. 6. XRD patterns of the composite fibers (PCLCS_mBG and PCLCS_nBG) were recorded before and after immersion in SBF solution for 7

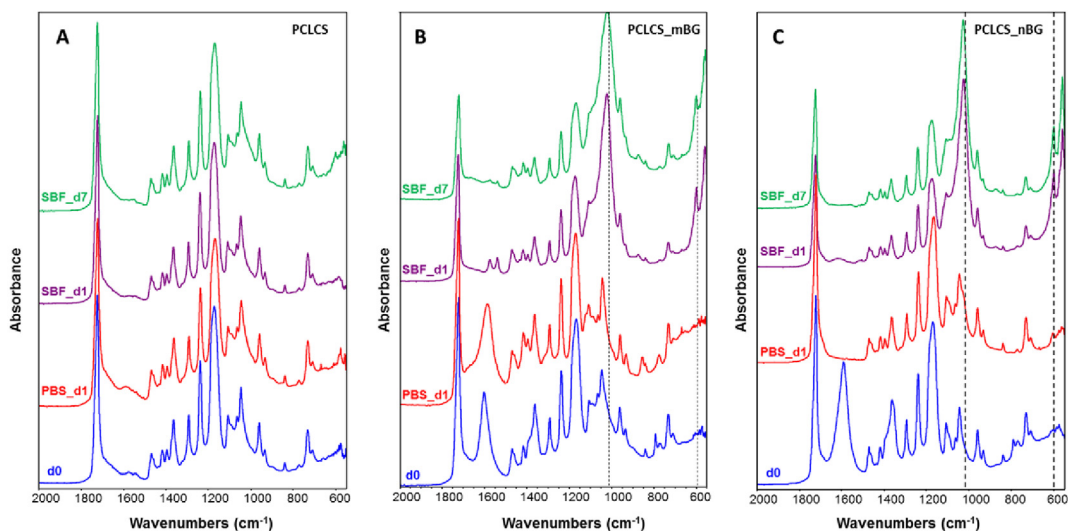


Fig. 9. FTIR spectra for the electrospun blend PCLCS (A), electrospun composites PCLCS_mBG (B) and PCLCS_nBG (C) before and after immersion in PBS for 1 day, in SBF for 3 days and 7 days.

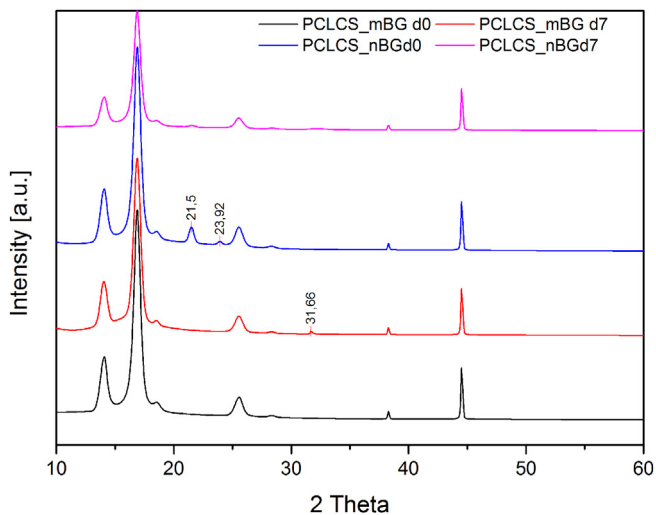


Fig. 10. XRD patterns of composite electrospun samples before and after immersion in SBF for 7 days.

Table 3

Mechanical properties of the electrospun blend and composite mats. UTS: ultimate tensile strength.

	PCLCS	PCLCS_nBG	PCLCS_mBG
Young's modulus (MPa)	3 ± 1	0.27 ± 0.04	0.7 ± 0.3
UTS Stress (MPa)	37 ± 21	7 ± 2	17 ± 11
Tensile strain (%)	31 ± 15	45 ± 12	28 ± 4

days and they are presented in Fig. 10. All patterns exhibit the main peaks measured also on the electrospun sample of neat PCL (pattern not shown). Slight modifications could be detected after immersion in SBF. In particular, the peaks at 2θ 21° and 24° decreased in intensity for the sample PCLCS_nBG, but no new peaks could be detected and related to the HCA layer. This could be explained by the fact that the amount of bioactive glass and related HCA deposition are negligible in comparison to the amount of PCL in the mats. For the composite sample PCLCS_mBG the only modification detected is related to the appearance of a new peak at 2θ 31°, which is ascribable to HCA [35,36].

3.4. Mechanical characterization

Uniaxial tensile tests were performed on the electrospun blend and composite mats. In Table 3, the values related to Young's modulus, ultimate tensile strength (UTS) and tensile strain are reported.

A reduction in the value of Young's modulus could be observed for both composites in comparison with the polymeric blend used as control. This decrease could be justified by the increase in the inhomogeneity in the average fiber diameter reported for both composites. This decrease, combined with the reduction in UTS values, could be explained by the high amount of inorganic particles in the polymeric blend fibers (30 wt% respect to the polymers amount). In fact, this amount is suitable for the preservation of sample bioactivity, but it is likely to be responsible for the brittle mechanical behavior of the composite samples. Reducing the amount of BG particles inside the composite meshes is likely to positively affect the mechanical properties of the composite meshes, where the particles would have a stiffening effect on the pliable matrix, however, the high bioactivity of the composite fibers

necessary for applications in bone tissue engineering needs to be preserved.

4. Conclusions

Two different sizes of BG particles were successfully embedded in electrospun PCL/chitosan nanofibrous mats. The morphological, chemical, mechanical and acellular bioactivity characterization was performed on both the polymeric and composite mesh structures. Benign solvents for electrospinning were used for fabrication of blend and composite mats. The optimized composite nanofibers showed deposition of HCA precipitates already after 1 day of immersion in SBF solution, confirming that the BG particles embedded in the polymeric meshes preserved their bioactivity. These results, combined with the other characterizations highlight the potential applications of the obtained mats as scaffolds for bone tissue engineering applications. Further detailed studies focused on cell viability are ongoing, which are required to complete the characterization of the composite nanofibers for the intended applications.

Acknowledgements

The authors thank Dr. D. Mohn and Prof. W. Stark (ETH Zurich) for providing the nanoscale bioactive glass powder used in this study. The authors thank Dr. J. Will for the support with XRD measurements. Liliana Liverani acknowledges funding from the European Union's Horizon 2020 research and innovation programme under the Marie Skłodowska-Curie grant agreement No 657264.

References

- [1] T. Jiang, E.J. Carbone, K.W.-H. Lo, C.T. Laurencin, Electrospinning of polymer nanofibers for tissue regeneration, *Prog. Polym. Sci.* 46 (2015) 1–24, <http://dx.doi.org/10.1016/j.progpolymsci.2014.12.001>.
- [2] B. Sun, Y.Z. Long, H.D. Zhang, M.M. Li, J.L. Duval, X.Y. Jiang, H.L. Yin, Advances in three-dimensional nanofibrous macrostructures via electrospinning, *Prog. Polym. Sci.* 39 (2014) 862–890, <http://dx.doi.org/10.1016/j.progpolymsci.2013.06.002>.
- [3] Y.-Z. Cai, G.-R. Zhang, L.-L. Wang, Y.-Z. Jiang, H.-W. Ouyang, X.-H. Zou, Novel biodegradable three-dimensional macroporous scaffold using aligned electrospun nanofibrous yarns for bone tissue engineering, *J. Biomed. Mater. Res. A* 100 (2012) 1187–1194, <http://dx.doi.org/10.1002/jbm.a.34063>.
- [4] D. Kai, S.S. Liow, X.J. Loh, Biodegradable polymers for electrospinning: towards biomedical applications, *Mater. Sci. Eng. C. Mater. Biol. Appl.* 45 (2014) 659–670, <http://dx.doi.org/10.1016/j.msec.2014.04.051>.
- [5] V. Pillay, C. Dott, Y.E. Choonara, C. Tyagi, L. Tomar, P. Kumar, L.C. Toit, V.M.K. Ndesendo, A Review of the Effect of Processing Variables on the Fabrication of Electrospun Nanofibers for Drug Delivery Applications, 2013 (2013) 22, <http://dx.doi.org/10.1155/2013/789289>.
- [6] S.L. Shenoy, W.D. Bates, H.L. Frisch, G.E. Wnek, Role of chain entanglements on fiber formation during electrospinning of polymer solutions: good solvent, non-specific polymer-polymer interaction limit, *Polym. Guildf.* 46 (2005) 3372–3384, <http://dx.doi.org/10.1016/j.polymer.2005.03.011>.
- [7] T. Jarusuwannapoom, W. Hongrojanawiat, S. Jitjicham, L. Wannatong, M. Nithitanakul, C. Pattamaprom, P. Koombhongse, R. Rangkupan, P. Supaphol, Effect of solvents on electro-spinnability of polystyrene solutions and morphological appearance of resulting electrospun polystyrene fibers, *Eur. Polym. J.* 41 (2005) 409–421, <http://dx.doi.org/10.1016/j.eurpolymj.2004.10.010>.
- [8] J. Sun, K. Bubel, F. Chen, T. Kissel, S. Agarwal, A. Greiner, Nanofibers by green electrospinning of aqueous suspensions of biodegradable block copolyesters for applications in medicine, pharmacy and agriculture, *Macromol. Rapid Commun.* 31 (2010) 2077–2083, <http://dx.doi.org/10.1002/marc.201000379>.
- [9] S. Agarwal, A. Greiner, On the way to clean and safe electrospinning-green electrospinning: emulsion and suspension electrospinning, *Polym. Adv. Technol.* 22 (2011) 372–378, <http://dx.doi.org/10.1002/pat.1883>.
- [10] K.H. Lee, H.Y. Kim, M.S. Khil, Y.M. Ra, D.R. Lee, Characterization of nano-structured poly(ϵ -caprolactone) nonwoven mats via electrospinning, *Polym. Guildf.* 44 (2003) 1287–1294, [http://dx.doi.org/10.1016/S0032-3861\(02\)00820-0](http://dx.doi.org/10.1016/S0032-3861(02)00820-0).
- [11] J.L. Ferreira, S. Gomes, C. Henriques, J.P. Borges, J.C. Silva, Electrospinning polycaprolactone dissolved in glacial acetic acid: fiber production, nonwoven characterization, and in vitro evaluation, *J. Appl. Polym. Sci.* 41068 (2014)

- 37–39, <http://dx.doi.org/10.1002/app.41068>.
- [12] G.R. Da Silva, T.H. Lima, R.L. Oréfice, G.M. Fernandes-Cunha, A. Silva-Cunha, M. Zhao, F. Behar-Cohen, In vitro and in vivo ocular biocompatibility of electrospun poly(ϵ -caprolactone) nanofibers, *Eur. J. Pharm. Sci.* 73 (2015) 9–19, <http://dx.doi.org/10.1016/j.ejps.2015.03.003>.
- [13] S. Soliman, S. Sant, J.W. Nichol, M. Khabiry, E. Traversa, A. Khademhosseini, Controlling the porosity of fibrous scaffolds by modulating the fiber diameter and packing density, *J. Biomed. Mater. Res. Part A* 96A (2011) 566–574, <http://dx.doi.org/10.1002/jbm.a.33010>.
- [14] A. Gholipour Kanani, S.H. Bahrami, Effect of changing solvents on poly(ϵ -caprolactone) nanofibrous webs morphology, *J. Nanomater.* 2011 (2011) 1–10, <http://dx.doi.org/10.1155/2011/724153>.
- [15] L. Van Der Schueren, B. De Schoenmaker, Ö.I. Kalaoglu, K. De Clerck, An alternative solvent system for the steady state electrospinning of polycaprolactone, *Eur. Polym. J.* 47 (2011) 1256–1263, <http://dx.doi.org/10.1016/j.eurpolymj.2011.02.025>.
- [16] C.J. Luo, E. Stride, M. Edirisinghe, Mapping the influence of solubility and dielectric constant on electrospinning polycaprolactone solutions, *Macromolecules* 45 (2012) 4669–4680, <http://dx.doi.org/10.1021/ma300656u>.
- [17] D. Dippold, A. Cai, M. Hardt, A.R. Boccaccini, R. Horch, J.P. Beier, D.W. Schubert, Novel approach towards aligned PCL-Collagen nanofibrous constructs from a benign solvent system, *Mater. Sci. Eng. C* 72 (2017) 278–283, <http://dx.doi.org/10.1016/j.msec.2016.11.045>.
- [18] R.A.A. Muzzarelli, F. Greco, A. Busilacchi, V. Sollazzo, A. Gigante, Chitosan, hyaluronan and chondroitin sulfate in tissue engineering for cartilage regeneration: a review, *Carbohydr. Polym.* 89 (2012) 723–739, <http://dx.doi.org/10.1016/j.carbpol.2012.04.057>.
- [19] K.T. Shalumon, K.H. Anulekha, C.M. Girish, R. Prasanth, S.V. Nair, R. Jayakumar, Single step electrospinning of chitosan/poly(caprolactone) nanofibers using formic acid/acetone solvent mixture, *Carbohydr. Polym.* 80 (2010) 414–420, <http://dx.doi.org/10.1016/j.carbpol.2009.11.039>.
- [20] E. Mirzaei, R. Faridi-Majidi, M.A. Shokrgozar, F. Asghari, Genipin cross-linked electrospun chitosan-based nanofibrous mat as tissue engineering scaffold, *Nanomed. J.* 1 (2014) 137–146, <http://dx.doi.org/10.7508/nmj.2014.03.003>.
- [21] L. Liverani, J.A. Roether, A.R. Boccaccini, Nanofiber composites in bone tissue engineering, in: M. Ramalagam, S. Ramakrishna (Eds.), *Nanofiber Compos. Mater. Biomed. Appl.*, 2016.
- [22] S.Ö. Gönen, M.E. Taygun, S. Küçükbayrak, Fabrication of bioactive glass containing nanocomposite fiber mats for bone tissue engineering applications, *Compos. Struct.* 138 (2016) 96–106, <http://dx.doi.org/10.1016/j.compstruct.2015.11.033>.
- [23] L. Liverani, A. Boccaccini, Versatile production of poly(epsilon-caprolactone) fibers by electrospinning using benign solvents, *Nanomaterials* 6 (2016) 75, <http://dx.doi.org/10.3390/nano6040075>.
- [24] W.C. Lepry, S. Smith, L. Liverani, A.R. Boccaccini, S.N. Nazhat, Acellular bioactivity of sol-gel derived borate glass-polycaprolactone electrospun scaffolds biomedical glasses, *Biomed. Glas.* 2 (2016) 88–98, <http://dx.doi.org/10.1515/bglass-2016-0011>.
- [25] L. Van Der Schueren, I. Steyaert, B. De Schoenmaker, K. De Clerck, Polycaprolactone/chitosan blend nanofibres electrospun from an acetic acid/formic acid solvent system, *Carbohydr. Polym.* 88 (2012) 1221–1226, <http://dx.doi.org/10.1016/j.carbpol.2012.01.085>.
- [26] T.J. Brunner, R.N. Grass, W.J. Stark, Glass and bioglass nanopowders by flame synthesis, *Chem. Commun. (Camb)* 305 (2006) 1384–1386, <http://dx.doi.org/10.1039/b517501a>.
- [27] M. Mačković, A. Hoppe, R. Detsch, D. Mohn, W.J. Stark, E. Spiecker, A.R. Boccaccini, Bioactive glass (type 45S5) nanoparticles: in vitro reactivity on nanoscale and biocompatibility, *J. Nanopart. Res.* 14 (2012), <http://dx.doi.org/10.1007/s11051-012-0966-6>.
- [28] T. Kokubo, H. Takadama, How useful is SBF in predicting in vivo bone bioactivity? *Biomaterials* 27 (2006) 2907–2915, <http://dx.doi.org/10.1016/j.biomaterials.2006.01.017>.
- [29] M. Cerruti, D. Greenspan, K. Powers, Effect of pH and ionic strength on the reactivity of bioglass 45S5, *Biomaterials* 26 (2005) 1665–1674, <http://dx.doi.org/10.1016/j.biomaterials.2004.07.009>.
- [30] T. Elzein, M. Nasser-Eddine, C. Delaite, S. Bistac, P. Dumas, FTIR study of polycaprolactone chain organization at interfaces, *J. Colloid Interface Sci.* 273 (2004) 381–387, <http://dx.doi.org/10.1016/j.jcis.2004.02.001>.
- [31] K. Zheng, A. Solodovnyk, W. Li, O.-M. Goudouri, C. Stähli, S.N. Nazhat, A.R. Boccaccini, Aging time and temperature effects on the structure and bioactivity of gel-derived 45S5 glass-ceramics, *J. Am. Ceram. Soc.* 98 (2015) 30–38, <http://dx.doi.org/10.1111/jace.13258>.
- [32] L. Tortora, Concolato, M. Urbini, S.M. Giannitelli, F. Basoli, A. Rainer, M. Trombetta, M. Orsini, P. Mozetic, Functionalization of poly(ϵ -caprolactone) surface with lactose-modified chitosan via alkaline hydrolysis: ToF-SIMS characterization, *Biointerphases* 11 (2016), <http://dx.doi.org/10.1116/1.4942498>, 02A323-1 – 02A323-10.
- [33] N. Noor Aliah, M.N.M. Ansari, Thermal analysis on characterization of polycaprolactone (PCL) – chitosan scaffold for tissue engineering, *Int. J. Sci. Res. Eng. Technol. (IJSRET)* 6 (2017) 2278–2882.
- [34] J.Y. Liu, L. Reni, Q. Wei, J.L. Wu, S. Liu, Y.J. Wang, G.Y. Li, Fabrication and characterization of polycaprolactone/calcium sulfate whisker composites, *eXPRESS Polym. Lett.* 5 (2011) 742–752, <http://dx.doi.org/10.3144/expresspolymlett.2011.72>.
- [35] M.K. Joshi, A.P. Tiwari, H.R. Pant, B.K. Shrestha, H.J. Kim, C.H. Park, C.S. Kim, In situ generation of cellulose nanocrystals in polycaprolactone nanofibers: effects on crystallinity, mechanical strength, biocompatibility, and biomimetic mineralization, *ACS Appl. Mater. Interfaces* 7 (2015) 19672–19683, <http://dx.doi.org/10.1021/acsami.5b04682>.
- [36] P. Balasubramanian, J.A. Roether, D.W. Schubert, J.P. Beier, A.R. Boccaccini, Bi-layered porous constructs of PCL-coated 45S5 bioactive glass and electrospun collagen-PCL fibers, *J. Porous Mater.* 22 (2015) 1215–1226, <http://dx.doi.org/10.1007/s10934-015-9998-5>.